Efficient numerical techniques for flow simulation in bubble column reactors

D. Kuzmin and S. Turek

Institute of Applied Mathematics (LS III), University of Dortmund
Vogelpothsweg 87, D-44227 Dortmund, Germany

Abstract

A dynamic Euler-Euler model for gas-liquid flows subject to mass transfer and simultaneous chemical reaction is assembled. The bubble size distribution is computed from an equation governing the evolution of average bubble mass. High-performance finite element tools for numerical solution of the problem at hand are discussed. Computational results for the chemisorption of CO_2 into NaOH shed some light on the implications of reaction enhanced mass transfer in bubble columns and call for further research in this field.

1 Introduction

Over the past decade, substantial progress has been made in numerical simulation of inert bubble columns. However, the literature concerning investigation of bubble columns in a reactive environment has been very scarce. In this paper, we present a fairly simple two-phase flow model which does bring mass transfer and chemical reactions into the picture [2]. It is based on an Euler-Euler formulation and allows for changes in the bubble size distribution, so that the bubbles may shrink due to gas dissolution and expand due to the fall of hydrostatic pressure.

As a recent European project ADMIRE (Advanced Design Methods for Improved Performance of Industrial Gas-Liquid Reactors) has demonstrated, commercial CFD codes like CFX-4 can be successfully applied to transient flows in gas-liquid reactors. However, realistic 3D simulations require prohibitively long computational times. Another source of concern is that no analysis of the accuracy of employed numerical schemes seems to be available. It was shown in [1] that a good agreement with experimental data can be misleading if the simulation results are corrupted by spurious numerical diffusion. Therefore, validation of a mathematical model is impossible without simultaneous validation of the numerical algorithm.

Our current research focuses on the development of robust and efficient solution techniques for multiphase flows. A high caliber of the numerical algorithm and computer implementation is a prerequisite for undertaking various (expensive) model extensions. We do not pursue the goal to develop a black-box routine suitable for all CFD problems at once. Instead, we try to design highly optimized solvers tailored to a specific problem and computer architecture. Each scheme is extensively tested on relevant benchmark problems and analyzed with respect to its stability and accuracy properties.

2 Physical assumptions

We consider an unsteady two-dimensional flow in a flat bubble column. For the time being, we use a constant effective viscosity and bubble path dispersion coefficients. However, a three-dimensional model with rigorous treatment of turbulence seems to be indispensable and will be implemented in the future. The liquid phase is assumed to be incompressible. The reactor is operated in dilute bubbly flow regime under isothermal conditions. Small spherical bubbles consist of a pure gas whose pressure and density are related by the ideal gas law: $p_G = \rho_G \frac{R}{\eta} T$. The local gas holdup is a function of the average bubble radius a and the number density n. We assume that there is no coalescence or breakup of bubbles, so that the number density is conserved:

$$\frac{\partial n}{\partial t} + \nabla \cdot (n \mathbf{v}_G) = 0. \tag{1}$$

3 Hydrodynamical model

The two-phase flow equations resemble their single-phase counterparts coupled by the interphase transfer terms responsible for the exchange of mass and momentum. The macroscopic continuity equations read

$$\frac{\partial \tilde{\rho}_G}{\partial t} + \nabla \cdot (\tilde{\rho}_G \mathbf{v}_G) = -4\pi a^2 n \eta \mathcal{N}, \tag{2}$$

$$\frac{\partial \tilde{\rho}_L}{\partial t} + \nabla \cdot (\tilde{\rho}_L \mathbf{v}_L) = 4\pi a^2 n \eta \mathcal{N}, \tag{3}$$

where $\tilde{\rho}_G = \epsilon \rho_G$ and $\tilde{\rho}_L = (1-\epsilon)\rho_L$ are the effective densities, and $\mathcal{N}$ is the molar flux of gas into the liquid (see below).

Conservation of momentum is given by

$$\tilde{\rho}_G \left(\frac{\partial \mathbf{v}_G}{\partial t} + (\mathbf{v}_G \cdot \nabla)\mathbf{v}_G \right) = -\epsilon \nabla p + \tilde{\rho}_G \mathbf{g} + \mathbf{f}_{\text{int}}, \tag{4}$$

$$\begin{aligned} \tilde{\rho}_L \left(\frac{\partial \mathbf{v}_L}{\partial t} + (\mathbf{v}_L \cdot \nabla)\mathbf{v}_L \right) &= -(1-\epsilon)\nabla p + \tilde{\rho}_L \mathbf{g} \\ &+ \nabla \cdot (\tilde{\mu}[\nabla \mathbf{v}_L + (\nabla \mathbf{v}_L)^T]) - \mathbf{f}_{\text{int}}, \end{aligned} \tag{5}$$

where $\tilde{\mu} = (1-\epsilon)\mu$ is the effective viscosity, and $\mathbf{g}$ is the gravitational force. It is common to assume that phases share the same pressure field $p = p_G = p_L$. The controversial interphase force term $\mathbf{f}_{\text{int}}$ involves contributions from the drag force, the virtual mass force and the lift force. Momentum transfer due to gas dissolution can be neglected.

It is worthwhile to reduce the presented two-phase flow model to a form amenable to numerical solution. Since the density of liquid is much greater than that of gas, the inertia and gravity terms in the gas phase momentum balance can be omitted

$$0 = -\epsilon \nabla p + \mathbf{f}_{\text{int}}. \tag{6}$$

If we add this equation to the liquid phase momentum balance, the interphase force term vanishes. The gradients of effective density create buoyancy forces which lead to

circulating flows in the liquid phase. Following Eigenberger and Sokolichin [1], we use an analog of the Boussinesq approximation for natural convection problems and drop the tilde everywhere except for the gravity term. In addition, the liquid phase continuity equation is replaced by the standard incompressibility constraint. After these modifications, we recover the standard Navier-Stokes equations with an extra buoyancy term proportional to the gas holdup

$$\frac{\partial \mathbf{v}_L}{\partial t} + (\mathbf{v}_L \cdot \nabla)\mathbf{v}_L = -\nabla P + \nu \Delta \mathbf{v}_L - \epsilon \mathbf{g}, \tag{7}$$

$$\nabla \cdot \mathbf{v}_L = 0, \qquad P = \frac{p - p_{\text{atm}}}{\rho_L} - g(h - \mathbf{k} \cdot \mathbf{x}). \tag{8}$$

According to Eigenberger and Sokolichin, this approximation is accurate at gas holdups less than 5%. It has another advantage that it is not necessary to deal with evolution of the free boundary on top of the bubble column.

The gas phase velocity is computed from a dispersive slip relation

$$\mathbf{v}_G = \mathbf{v}_L + \mathbf{v}_{\text{slip}} + \mathbf{v}_{\text{disp}}, \tag{9}$$

where $\mathbf{v}_{\text{slip}}$ is the standard slip velocity implied by (6). Bubble path dispersion is taken into account by $\mathbf{v}_{\text{disp}}$ which is proportional to the gas holdup gradient and generally to the turbulent eddy viscosity of the liquid phase [2].

The effective density of the gas phase can be represented as the product of the average bubble mass and the number density

$$\tilde{\rho}_G = mn. \tag{10}$$

Substituting this expression into equation (2) and using (1), we derive an equation for evolution of the bubble mass [2]

$$\frac{\partial m}{\partial t} + \mathbf{v}_G \cdot \nabla m = -4\pi a^2 \eta \mathcal{N}. \tag{11}$$

Then the associated bubble radius is given by

$$a = \sqrt[3]{\frac{3}{4}\frac{m}{\pi \rho_G}} = \sqrt[3]{\frac{3}{4}\frac{mRT}{\pi p \eta}}. \tag{12}$$

The gas holdup distribution follows from the relation $\epsilon = \frac{4}{3}\pi a^3 n$.

4 Mass transfer and chemical reactions

The dissolved gas is involved in second-order chemical reactions in the liquid phase. The equations for effective concentrations of species read:

$$\frac{\partial \tilde{c}_A}{\partial t} + \nabla \cdot (\tilde{c}_A \mathbf{v}_L) = \nabla \cdot (\tilde{D}_A \nabla c_A) - \tilde{k}_2 c_A c_B + 4\pi a^2 n \mathcal{N}, \tag{13}$$

$$\frac{\partial \tilde{c}_B}{\partial t} + \nabla \cdot (\tilde{c}_B \mathbf{v}_L) = \nabla \cdot (\tilde{D}_B \nabla c_B) - \nu_B \tilde{k}_2 c_A c_B, \tag{14}$$

$$\frac{\partial \tilde{c}_P}{\partial t} + \nabla \cdot (\tilde{c}_P \mathbf{v}_L) = \nabla \cdot (\tilde{D}_P \nabla c_P) + \nu_P \tilde{k}_2 c_A c_B. \tag{15}$$

The rate of interphase mass transfer is proportional to the interfacial area exposed per unit volume and the difference between concentration of dissolved gas at the interface and in the bulk liquid. According to the empirical Henry's law, the interfacial concentration is in equilibrium with the gas pressure: $p_G = Hc_A^*$. The molar flux of gas is calculated by the two-film theory: $\mathcal{N} = Ek_L^0(c_A^* - c_A)$. Since the gas is pure, there is no resistance to mass transfer on the gas side. Correction to the liquid-side mass transfer coefficient k_L^0 due to chemical reaction is represented by the enhancement factor E.

5 Numerical algorithm

The employed numerical algorithm is based on a finite element discretization and makes an extensive use of operator-splitting tools. To put it another way, the original initial/boundary value problem is reformulated as a sequence of simpler subproblems which are treated separately by appropriately designed numerical schemes. Different time stepping is used for different subproblems if this is dictated by stability or accuracy considerations. A high-performance software package FEATFLOW lends itself to computation of the velocity and pressure fields by means of the Multilevel Pressure Schur Complement techniques [3]. The FEATFLOW framework originally developed for single-phase incompressible flows offers a wide range of state-of-the-art numerical ingredients such as optimized multigrid solvers, adaptive fixed-point defect correction approach for the nonlinearity, automatic time step control and novel iterative filtering techniques for handling complex geometries and moving boundaries. In our experience, these methods exhibit excellent performance for a variety of industrial applications in aerodynamics, acoustics, non-Newtonian fluids, heat transfer and fluid-structure interaction to name just a few. Now they are being extended to multiphase flow simulations.

The problems for transport of scalar quantities require special treatment, since conventional discretization schemes fail when convection dominates, while upwind-like methods suffer from excessive numerical diffusion. A proper remedy is provided by high-order Taylor-Galerkin schemes which are characterized by the absence of any free or adjustable parameter. The enhanced stability follows naturally from an improved temporal approximation. However, it is known that high-order schemes are prone to producing spurious undershoots and overshoots in proximity to discontinuities. Sometimes the wiggles can be tolerated, but here we may end up having negative concentrations or gas holdups, which is clearly unacceptable. In order to get rid of oscillations, we resort to a finite element counterpart of the flux-corrected transport procedure (FEM-FCT). The essence of flux limiting is the replacement of a formally high-order method by a monotone low-order method near discontinuities, where non-physical oscillations are likely to arise. The resulting numerical solution is monotonicity-preserving and enjoys a sharp resolution of shocks and contact discontinuities.

Hardware-specific optimization of software can yield a dramatic gain in efficiency. This issue will be addressed within the FEAST project which was launched to update FEATFLOW with special emphasis on: (closer to) peak performance on modern and future processors, hierarchical data structures, robust and efficient multigrid behavior, low storage requirements and parallelization tools directly included on low level. Recent tests with matrix-vector applications on different computer platforms have shown that standard techniques implemented in many commercial and academic codes are far from

being optimal. Hence, the available computing power cannot be duly utilized, so that the performance of one processor in a supercomputer is comparable with that of a home PC.

6 Computational results

To give an insight into the complex interplay of hydrodynamic processes and mass transfer/reaction phenomena in bubble columns, we present selected simulation results. Bubbles consisting of pure carbon dioxide are continuously fed at the bottom of the reactor. The gas is gradually absorbed into the liquid phase where it may react with sodium hydroxide supplied in a batch mode: $CO_2 + 2NaOH \rightarrow Na_2CO_3 + H_2O$.

Let us first consider the startup behavior of a locally aerated bubble column. Carbon dioxide is highly soluble in water, so the bubble radius at the outlet falls short of its value at the inlet even in the case of physical absorption when the gas dissolves without reacting. Nevertheless, the rising bubbles produce a pronounced liquid circulation and, consequently, an intensive mixing in the reactor. Figure 1 shows instantaneous concentration fields for the dissolved carbon dioxide during the first minute after the beginning of aeration. Chemical reaction may accelerate mass transfer to the extent that the bubbles are completely dissolved in the vicinity of the inlet. In this case, circulation takes place only in the lower part of the reactor, and the distribution of produced sodium carbonate assumes snail-like shapes depicted in Figure 2.

Now let us turn to investigation of fast reaction in a uniformly aerated bubble column. At low gas throughputs, the bubbles rise uniformly so that there is no liquid circulation in the reactor. Such flow regime is known as homogeneous. Sharp bubble and reaction fronts are observed in this case. The lifetime of a bubble is very small, and the reaction product is layered at the bottom of the bubble column. At high gas throughputs, the two-phase flow switches over to the so-called heterogeneous regime. The gas holdup profiles are no longer flat, and vortices are generated close to the gas distributor. They spread sodium carbonate as shown in Figure 3.

These examples demonstrate the crucial role played by the bubble size distribution in gas-driven bubble columns. Clearly, a more realistic model must also provide for coalescence and breakup of bubbles. This can be accomplished on the basis of population balances if the numerical algorithm is efficient enough to handle a certain number of additional equations resulting from discretization of the spectrum of possible bubble masses.

References

[1] G. Eigenberger and A. Sokolichin, Modellierung und effiziente numerische Simulation von Gas-Flüssigkeits-Reaktoren mit Blasenströmungen nach dem Euler-Euler-Konzept. DFG-Zwischenbericht (1995–1997), *http://pcvt12.verfahrenstechnik.uni-stuttgart.de/alex/icvt2.html*.

[2] D. Kuzmin, *Numerical Simulation of Reactive Bubbly Flows.* Dissertation, Jyväskylä Studies in Computing, 1999.

[3] S. Turek, *Efficient Solvers for Incompressible Flow Problems: An Algorithmic and Computational Approach*, LNCSE 6, Springer, 1999.

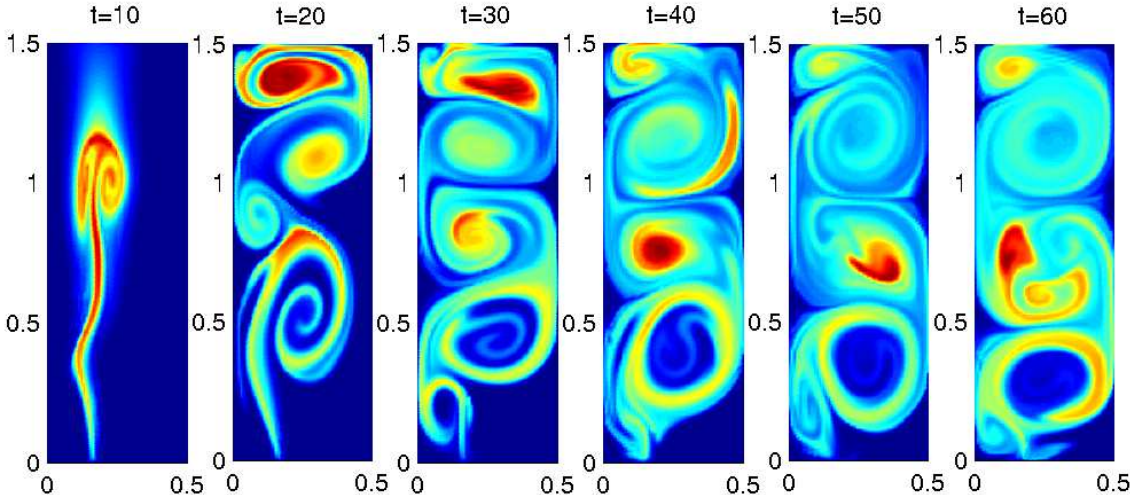

Figure 1. LABC: CO_2, $w_G = 0.18\ mm/s$, physical absorption.

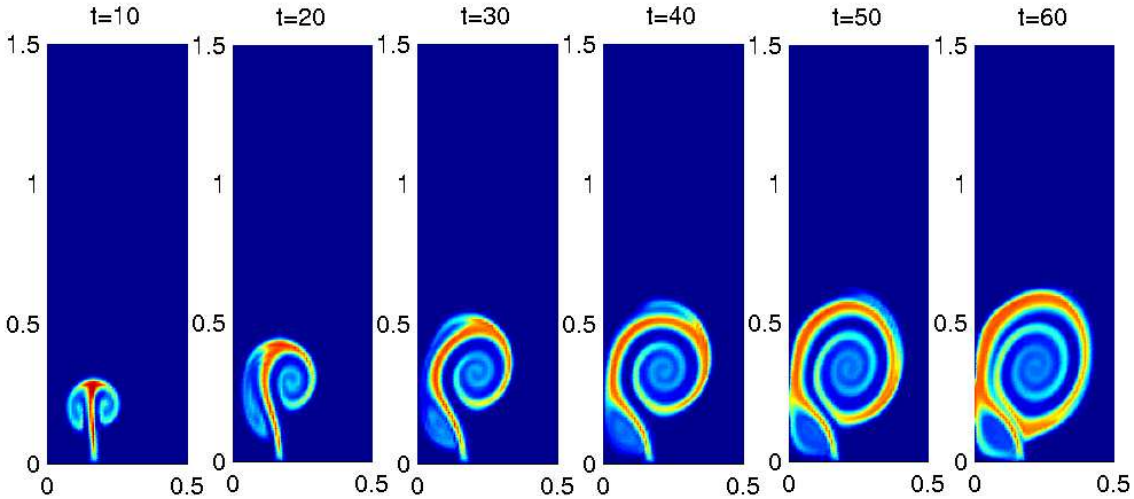

Figure 2. LABC: Na_2CO_3, $w_G = 0.18\ mm/s$, $c^0_{\mathrm{NaOH}} = 1\ mol/l$.

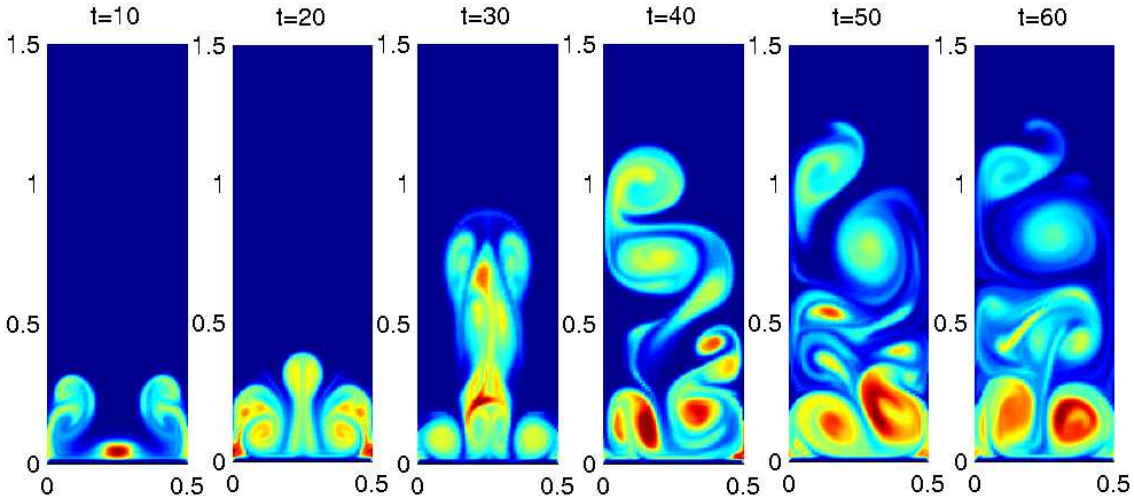

Figure 3. UABC: Na_2CO_3, $w_G = 2\ cm/s$, $c^0_{\mathrm{NaOH}} = 1\ mol/l$.